

¹ **Population dynamics of a globally rare yet locally abundant endemic**

² **monocarpic perennial (*Oenoethera coloradensis*)**

³ Alice E. Stears^{1*}, Bonnie Heidel², Maria Paniw³, Roberto Salguero-Gómez⁴, Daniel C.

⁴ Laughlin¹

⁵ ¹Botany Department and Program in Ecology, University of Wyoming, Laramie, WY;

⁶ ²Wyoming Natural Diversity Database, University of Wyoming, Laramie, WY;

⁷ ³Estación Biológica de Doñana, Sevilla, Spain;

⁸ ⁴Department of Zoology, University of Oxford, Oxford, OX2 6LD, United Kingdom

⁹ *Corresponding Author: astears@uwyo.edu

¹⁰ **Keywords:** population dynamics, rare species, integral projection models,

¹¹ **Abstract**

¹² 1. The long-term persistence of rare species has long been a motivating ques-
¹³ tion for ecologists. Classical theory implies that community dynamics should be
¹⁴ driven by common species, and that natural selection should not allow small pop-
¹⁵ulations of rare species to persist. Yet, a majority of the species found on Earth
¹⁶ are rare. Consequently, several mechanisms have been proposed to explain their
¹⁷ persistence, including negative density dependence, demographic compensation,
¹⁸ vital rate buffering, asynchronous responses of subpopulations to environmental
¹⁹ heterogeneity, and fine-scale source-sink dynamics. Persistence of seeds in a seed-
²⁰ bank, which is often ignored in models of population dynamics, can also buffer
²¹ small populations against collapse.

²² 2. We use integral projection models (IPMs) to examine the population dynam-
²³ ics of *Oenothera coloradensis*, a rare, monocarpic perennial forb, and determine

whether any of five proposed demographic mechanisms for rare species persistence contribute to the long-term viability of two populations. We also evaluate whether including a discrete seedbank stage improves population models for this species, and simulate population growth rate under different climate scenarios to assess the persistence outlook for *O. coloradensis* populations.

3. Including a seedbank stage in population models has a significant negative impact on modeled *O. coloradensis* population growth rate. IPMs that included a discrete seedbank state suggest that negative density-dependence is acting to maintain positive growth rates. We do not identify evidence of any other proposed mechanisms of rare species persistence.

4. *Synthesis:* IPMs of two populations of the rare species *O. coloradensis* emphasize the importance of including cryptic life stages such as seedbanks in demographic models, but fail to provide strong support for most of the proposed mechanisms of rare species persistence. We propose that high micro-site abundance enables this species to persist, allowing it to sidestep the demographic and genetic challenges of small population size that rare species typically face. These results support the idea that globally rare species can be locally abundant, and reinforce that uniform strategies of management and conservation will not equally benefit all rare species.

43 Introduction

44 Determining how and why populations of rare species persist has motivated ecological
45 research since its inception (Levins & Culver, 1971; Drury, 1974). Theoretically, low pop-

ulation size is a final step on a trajectory toward extinction (Stanley, 1979; Rosenzweig & Lomolino, 1997) or the first step toward ubiquity (Spear, Walsh, Ricciardi, & Vander Zanden, 2021). Yet, small but stable populations of rare species exist in every ecosystem and taxonomic group (Magurran & Henderson, 2011). In fact, a large proportion of species globally – as many as 35% of plant species, for example— can be considered naturally rare (Enquist et al., 2019). The prevalence of rarity suggests it is an evolutionarily stable strategy rather than a stop along the path toward extinction or invasion, and implies that there must be both fundamental and realized niches that are available for rare species to occupy. A growing body of evidence demonstrates the importance of rare species to biological processes. For example, species-specific perturbations of rare species population dynamics have a disproportionate adverse impact on community stability (Arnoldi, Loreau, & Haegeman, 2019; Säterberg, Jonsson, Yearsley, Berg, & Ebenman, 2019). The presence and abundance of rare species can also significantly alter community functional composition (Leitão et al., 2016; Burner et al., 2022), which in turn impacts ecosystem function (Lyons, Brigham, Traut, & Schwartz, 2005).

Effective conservation and management of rare species require a detailed understanding of both the conditions causing rarity initially, and the mechanisms that allow rare species to persist. Causes of rarity can vary from highly-specific habitat requirements (Sgarbi & Melo, 2018), to adverse impacts of anthropogenic environmental change. In order to then persist in a state of rarity, a species must overcome any of multiple potential challenges, primarily the negative effects of demographic, environmental, and genetic stochasticity (random variation in vital rates (e.g., survival, reproduction), abiotic conditions, and genetic allele frequencies (May, 1973)). Stochastic deleterious events can cause extirpation or even

69 extinction of rare species, since there may not be enough unaffected individuals or subpop-
70 ulations to “rescue” the affected population(Nei, Maruyama, & Chakraborty, 1975). Rare
71 species that maintain populations over time typically do so by employing demographic strate-
72 gies that compensate for the adverse effects of small population size. There are five main
73 strategies that allow persistence of rare populations (Fig. 1) (Dibner, Peterson, Louthan, &
74 Doak, 2019): negative density-dependence (Rovere & Fox, 2019), demographic compensa-
75 tion (Villellas, Doak, García, & Morris, 2015), vital rate buffering (Pfister, 1998; Hilde et al.,
76 2020), asynchronous responses between subpopulations (Abbott, Doak, & Peterson, 2017),
77 and fine-scale source-sink dynamics (Kauffman, Pollock, & Walton, 2004; Pulliam, 2016).
78 Negative density-dependence occurs when the growth rate (λ) of a population increases at
79 smaller population size. Demographic compensation occurs when different vital rates are
80 affected in opposing ways by the same perturbation in the environment, which can help
81 maintain a relatively constant population λ in response to environmental variation. Vital
82 rate buffering occurs when the variability of vital rates decreases as the vital rate becomes
83 more important (i.e., has a higher elasticity) for population growth rate, which prevents
84 the negative effects of temporal variation on the deterministic λ across time (Tuljapurkar,
85 1989). Spatial asynchrony occurs when subpopulations close to one another have different or
86 even opposing growth rates, resulting in a stable population-wide λ . Fine-scale source-sink
87 dynamics occur when there is gene flow between subpopulations that bolsters the size and
88 genetic diversity of very small subpopulations, which again results in a stable population-
89 level λ . Each of these mechanisms can act independently, but also can interact or overlap
90 with other mechanisms (Dibner et al., 2019).

91 Here, to identify which mechanisms are contributing to the persistence or even popula-

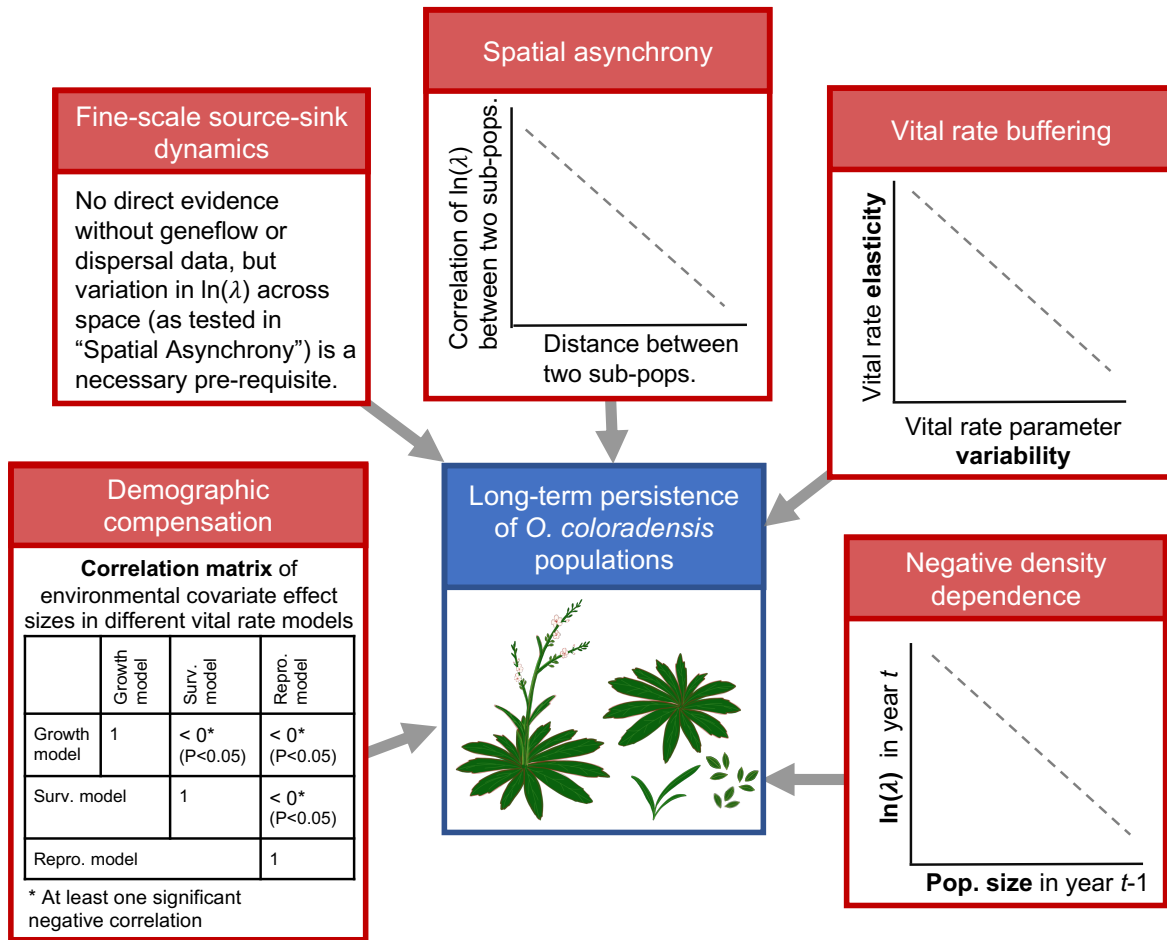


Figure 1: The evidence that would be required to show support for each of the five mechanisms that can contribute to the long-term viability of small populations of rare species.

92 tion growth of a rare, endemic plant species, *Oenothera coloradensis* (Onagraceae), we use
 93 integral projection models (IPMs) (Easterling, Ellner, & Dixon, 2000) that include a dis-
 94 crete seedbank population state. IPMs are flexible models of population dynamics that are
 95 constructed using regression models that describe vital rate change across a continuous state
 96 variable such as size. IPMs have multiple advantages over traditional matrix models, includ-
 97 ing better performance with small datasets (Ramula, Rees, & Buckley, 2009), and simple
 98 incorporation of covariates of interest directly into vital rate models. Our first objective was

99 to determine if including information about the seedbank significantly altered population
100 models for *O. coloradensis*. Seedbanks can serve as important reservoirs of genetic diversity
101 and buffer populations against collapse (Vitalis, Glémin, & Olivieri, 2004; Jongejans, Shep-
102 pard, & Shea, 2006), and can be especially critical for monocarpic perennials that only flower
103 once in their lifetime (Rees et al., 2006). For these reasons, we expected that a soil seedbank
104 is important for *O. coloradensis*. Seedbanks are often not included in population models
105 because their parameters can be very difficult to estimate, but previous work shows that
106 including them can significantly alter model outcomes (Paniw, Quintana-Ascencio, Ojeda,
107 & Salguero-Gómez, 2017; Nguyen, Buckley, Salguero-Gómez, & Wardle, 2019). We pre-
108 dicted that including a discrete seedbank state in IPMs would increase the projected λ for
109 *O. coloradensis* populations.

110 Our second objective was to identify whether any of the five persistence mechanisms was
111 acting to maintain *O. coloradensis* populations. This species occurs in habitats that naturally
112 experience frequent, highly localized disturbance, which means that some subpopulations
113 of *O. coloradensis* might be negatively affected by flood, for example, while other nearby
114 populations are simultaneously thriving due to lack of disturbance. Additionally, previous
115 matrix population models constructed for this species in the 1990s found substantial variation
116 in lambda across space and time (Floyd & Ranker, 1998). The population-wide pattern of
117 asynchronous disturbance also could make source-sink dynamics important. We also have
118 evidence of large fluctuations in the number of plants within subpopulations (Heidel, Tuthill,
119 & Wallace, 2021), which indicate that population growth rate decreases at high population
120 size and increases at low population size. Therefore, we predicted that density dependence,
121 small-scale source-sink dynamics and asynchronous responses between subpopulations would

122 be important mechanisms of persistence for *O. coloradensis*.

123 **Methods**

124 **Species Description**

125 *Oenothera coloradensis* (Onagraceae) (Wagner, Hoch, & Raven, 2007) is an herbaceous,
126 monocarpic perennial plant species that primarily occurs in open, frequently disturbed habi-
127 tats with sub-irrigated, alluvial soils (Jennings, 2000). Non-reproductive individuals consist
128 of a rosette of basal leaves with a fleshy taproot. Flowering typically occurs after several
129 years of age around four years of age, when individuals produce a 10-30 cm long floral stalk.
130 Individuals almost always die after reproducing—93% of the time in populations we ob-
131 served. *O. coloradensis* populations typically occur within the floodplain of ephemeral or
132 perennial streams, but also exist in wet meadows, drainage bottoms, and spring-fed wetlands
133 (Munk, 1999). Relatively frequent disturbance such as flooding that reduces growth of both
134 woody and herbaceous species and removes litter is important for this species, especially for
135 successful seedling recruitment (Jennings, 2000; Burgess, 2003).

136 All historical and known extant *O. coloradensis* populations lie within a 7,000-hectare
137 area that includes southeast Wyoming, northern Colorado, and a small part of southwest
138 Nebraska (Fig. S1). The largest population on Federal land occurs on the F. E. Warren Air-
139 force Base near Cheyenne, WY (FEWAFB). The Soapstone Prairie Natural Area, a public
140 property owned by the city of Fort Collins, CO, has the largest documented number of *O.*
141 *coloradensis* individuals, but this population has not been routinely monitored (Jennings,
142 2000). Decline in a majority of the known populations between the mid-1980s and 2000

¹⁴³ lead the U.S. Fish and Wildlife Service (USFWS) to designate *O. coloradensis* as a “threat-
¹⁴⁴ ened” species protected under the Endangered Species Act (Jennings, 2000). Although this
¹⁴⁵ species appears to be naturally rare, managers were concerned that, without protection, *O.*
¹⁴⁶ *coloradensis* had the potential for extinction because of habitat loss due to ranching, natural
¹⁴⁷ resource extraction, and shrub encroachment resulting from altered disturbance regimes.

¹⁴⁸ Previous work established that *O. coloradensis* population growth rate is particularly
¹⁴⁹ impacted by recruitment of seedlings (Floyd & Ranker, 1998). Seedbanks are also likely
¹⁵⁰ important for the viability of this species, since years of high seedling density are not nec-
¹⁵¹ essarily preceded by years of high rates of flowering and seed production (Munk, Hild, &
¹⁵² Whitson, 2002). The *O. coloradensis* seedbank has not been studied directly, but a green-
¹⁵³ house seed viability and germination study showed that an average of 58% of seeds produced
¹⁵⁴ by a parent plant are viable, and that a viable seed has a 20% probability of germinating
¹⁵⁵ after two months of cold stratification (Burgess, Hild, & Shaw, 2005). These seed viability
¹⁵⁶ and germination rates did not change meaningfully over five years.

¹⁵⁷ More information about *O. coloradensis* can be found in the Supplementary Material:
¹⁵⁸ “Species Information.”

¹⁵⁹ **Demographic Data Collection**

¹⁶⁰ We conducted a three-year demographic study of *O. coloradensis* across six spatially
¹⁶¹ distinct subpopulations, three in the F.E. Warren Airforce Base (FEWAFB) population and
¹⁶² three at the Soapstone Prairie Natural Area population (Table S1; Fig. S1). In early summer
¹⁶³ 2018, we established three 2x2 m² quadrats in each of these subpopulations, resulting in 18
¹⁶⁴ plots (Table S1) (Unnamed creek, Crow creek, and Diamond creek at FEWAFB and Meadow,

165 Pasture HQ3 and Pasture HQ5 at Soapstone). Plants larger than 3 cm are typically "non-
166 seedling" plants at least one year in age. In each study plot, we tagged and mapped each
167 unique "non-seedling" individual and recorded longest leaf length, reproductive status, and
168 seed production for each. Individuals smaller than 3 cm in leaf length are typically seedlings
169 that germinated that year, occur at high density, and are less likely to survive than non-
170 seedling plants. Due to these factors, we tallied seedlings in each plot, but did not map or
171 tag them. In subsequent 2019 and 2020 censuses, we mapped and tagged new "non-seedling"
172 individuals, and re-measured all surviving individuals from previous years. Sample size in a
173 given year at a subpopulation ranged from 48 to 1527 individuals (Table S1). All mapping,
174 tagging, and leaf measurements took place between late May and early July, coinciding with
175 the peak of vegetative growth for this species.

176 It was not possible to measure seed production exactly because *O. coloradensis* seeds are
177 contained in indehiscent capsules. Additionally, buds on the same individual flower and set
178 seed with a time lag of up to several weeks, such that mature seed capsules often exist at
179 the tip of a stem while un-opened buds lower down on that same stem have not yet flowered.

180 This lag makes it difficult to count the total number of capsules produced by an individual.
181 However, seed capsules leave a noticeable scar on the stem, so we used the number of seed
182 capsule scars on reproductive stems as an estimate of capsule production. Counting scars
183 is extremely time-intensive since a single plant can produce several hundred capsules, so we
184 used Poisson generalized linear regression to estimate the relationship between the length
185 of stem bearing capsule scars and the number of capsules produced by that stem. Poisson
186 regression models fit to stem measurements and capsule counts from 106 individuals in 2018
187 indicates that the number of capsules produced by an individual (C) can be predicted by

188 $e^{(1.843+0.119\times S)}$, where S is the stem length in cm (pseudo R-squared = 0.42, $P = < 0.01$,
189 Residual deviance = 186.98, df = 104) (Fig. S2). We used this relationship to estimate
190 capsule production for each reproductive individual. Previous work indicated that each
191 capsule contained an average of 4 seeds, so we multiplied the estimated number of capsules
192 produced by an adult plant by 4 to estimate seed production (Burgess et al., 2005).

193 **Environmental Measurements**

194 To determine the effect of temporal variation in climate on *O. coloradensis* populations,
195 we used modeled, site-level temperature, and precipitation data from PRISM (PRISM Cli-
196 mate Group; Oregon State University, 2021), which we refer to as "environmental covariates".
197 We calculated the mean temperature of both the growing season and preceding winter season
198 for each year of demographic vital rate data collection at FEWAFB and Soapstone Prairie.
199 We also calculated total precipitation for each hydrological year, the period from October of
200 the previous year to September of the current year. We used this metric in place of growing
201 season precipitation because the shortgrass steppe ecosystem in which *O. coloradensis* oc-
202 curs receives a majority of its annual precipitation in the form of snow, and melting snow
203 from the previous winter likely contributes to springtime seedling recruitment. Average
204 temperature of the previous winter is also likely important for seedling recruitment, because
205 seed germination is triggered by cold stratification (Burgess et al., 2005). Growing season
206 temperature and precipitation are likely important for growth, survival, and reproductive
207 output of non-seedling plants.

208 Objective 1: Quantifying the Importance of the Seedbank Stage

209 *Population Models:* We used data from the demographic study detailed above in com-

210 bination with results from greenhouse and field seedbank studies to parameterize integral

211 projection models (IPMs) for *O. coloradensis*, which we then used to address each of the

212 objectives outlined in the Introduction. We first created a density-independent IPM using

213 data from both Soapstone and FEWAFB that had a single continuous, size-based population

214 state, and did not include a seedbank state (Table 1: IPM “A”). Then, we created a suite

215 of IPMs that included both a discrete seedbank state, and a continuous, size-based stage for

216 above-ground individuals (Table 1: IPMs “A” – “NN”) (Ellner & Rees, 2006; Rees et al.,

217 2006; Paniw et al., 2017). Each of these IPMs used a different subset of data, and included

218 different covariates in vital rate models. First, the data used to fit vital rate models came

219 either from a single subpopulation, a population (FEWAFB or Soapstone prairie), or from all

220 locations, and included data for both transitions, or only one transition (2018-2019 or 2019-

221 2020). Second, while all vital rate models included size in the current year (size_t) (or in some

222 cases when the model fitting process indicated, $(\text{size}_t)^2$) as a predictor of vital rates, these

223 models could also include predictor terms for any combination of the following: population

224 size in the previous year (to account for density dependence), environmental variation (water

225 year precipitation, mean annual growing season temperature, and mean annual winter tem-

226 perature), and a random intercept of subpopulation to approximate effects of demographic

227 stochasticity.

Table 1: A description of the data used to create each IPM, as well as the covariates included in the vital rate models used in that IPM. $\ln(\lambda)$ estimates and 95% bootstrap confidence intervals of $\ln(\lambda)$ are also shown for each IPM.

IPM	Data Included						Transition	Covariates	$\ln(\lambda)$ (95% CI)			
	Continuous state only		All subpopulations	Each pop.	Each subpop.							
	Continuous + seedbank state	All subpopulations			Unnamed Creek	Diamond Creek						
			Soapstone	FEWAFB	Crow Creek	Meadow	HQ3	HQ5				
A	x	x	x				x	All Transitions	0.27 (0.269, 0.271)			
B		x	x				x	2018-2019	0.65 (0.648, 0.650)			
C	x			x			x	2019-2020	0.48 (0.477, 0.489)			
D	x				x		x	Density dependence	1.13 (1.124, 1.142)			
E	x				x		x		0.74 (0.725, 0.746)			
F	x				x		x		0.54 (0.520, 0.551)			
G	x				x	x	x		0.395 (0.378, 0.401)			
H	x				x	x	x		0.53 (0.526, 0.540)			
I	x			x			x		0.59 (0.576, 0.637)			
J	x			x			x		0.63 (0.611, 0.723)			
K	x			x		x	x		-0.10 (-0.135, 0.063)			

L	x			x	x		x	-0.20 (-0.229, -0.167)
M	x			x	x		x	1.31 (1.294, 1.354)
N	x			x	x		x	2.31 (2.297, 2.33)
S	x		x	x	x	x	x	0.58
T	x		x	x	x	x	x	0.51
U	x		x	x	x	x	x	0.90
V	x		x	x	x	x	x	-0.27
W	x		x	x	x	x	x	-0.18
X	x		x	x	x	x	x	0.76
AA	x	x		x				0.50 (0.497, 0.501)
BB	x		x		x			0.73 (0.729, 0.733)
CC	x		x		x			0.38 (0.370, 0.388)
DD	x		x		x			1.56 (1.545, 1.572)
EE	x		x		x			0.90 (0.864, 0.904)
FF	x		x		x			0.62 (0.592, 0.637)
GG	x		x		x			0.73 (0.727, 0.753)
HH	x		x	x	x			1.11 (1.108, 1.126)
II	x		x		x			0.50 (0.492, 0.513)
JJ	x		x		x			0.71 (0.692, 0.726)
KK	x		x		x			0.76 (0.739, 0.774)
LL	x		x		x			0.41 (0.378, 0.448)
MM	x		x		x			0.03 (0.013, 0.040)
NN	x		x		x			-0.10 (-0.112, -0.097)

*Note: We did not calculate bootstrap 95% confidence intervals for $\ln(\lambda)$ of models “S” –“X”, since only vital rate parameters and not lambda values from these models were used in further analysis.

²²⁸ The IPM with one state variable corresponding to continuous plant size (IPM “A”) used
²²⁹ a kernel structure where the continuous, above-ground population state ($(n(z', t+1))$ at time
²³⁰ $t + 1$ was described by the following equation:

$$n(z', t+1) = \int_L^U (1 - P_b(z))s(z)G(z', z)n(z, t)dz + pEstab \int_L^U P_b(z)b(z)c_o(z')n(z, t)dz \quad (1)$$

²³¹ All of the IPMs with two population states used the same kernel structure, where the con-
²³² tinuous, above-ground population state ($(n(z', t+1))$) and the seedbank state ($B(t+1)$) at
²³³ time $t + 1$ were described by the following equations:

$$n(z', t+1) = \int_L^U (1 - P_b(z))s(z)G(z', z)n(z, t)dz + goCont \int_L^U P_b(z)b(z)c_o(z')n(z, t)dz + outSB \quad (2)$$

$$B(t+1) = goSB \int_L^U P_b(z)b(z)n(z, t)dz + B(t)staySB \quad (3)$$

²³⁵ In both sets of equations, z is the distribution of plant longest leaf length in the current
²³⁶ year (“ $size_t$ ”), z' is the distribution of plant size in the next year (“ $size_{t+1}$ ”), and U and
²³⁷ L are the upper and lower boundaries of plant size. $G(z', z)$ is the vital rate function
²³⁸ describing $size_{t+1}$ as a function of $size_t$. The vital rate functions $s(z)$, $Pb(z)$, and $b(z)$
²³⁹ describe the relationship between $size_t$ and survival probability of non-flowering plants,
²⁴⁰ flowering probability, and seed production of flowering plants, respectively. $c_o(z')$ is the
²⁴¹ distribution of above-ground recruit $size_{t+1}$. $goCont$, $outSB$, $goSB$, and $staySB$ are discrete

parameters that determine seedbank dynamics. $goCont$ is the probability of a seed produced in year t germinating as a seedling in year $t + 1$, $outSB$ is the probability of a seed from the seedbank in year t germinating as a seedling in year $t + 1$, $goSB$ is the probability of a seed produced in year t going into the seedbank in year $t + 1$, and $staySB$ is the probability of a seed from the seedbank in year t persisting in the seedbank in year $t + 1$ (Paniw et al., 2017) (Table 2). $pEstab$ is the probability of a seed produced in year t establishing as a seedling in year $t + 1$.

We used data from the three-year demographic monitoring study to parameterize the vital rates used in the IPMs (vital rates are shown in Fig. 2). Vital ratefunctions for the continuous, size-based above-ground stage were parameterized using data from “non-seedling plants” as well as seedlings. Although seedlings (above-ground plants < 3 cm in leaf length) were only tallied in each subplot of each quadrat and year instead of tagged and measured, we incorporated them into the dataset for continuous, above-ground plants by assigning them a random size drawn from a continuous, uniform probability distribution (seedling size $\sim U(0.1, 3)$). Each new recruit to the > 3 cm stage in year $t + 1$ was randomly assigned to a seedling within the same subplot in year t . Seedlings in year t that were assigned a recruit in year $t + 1$ survived, while those without an assigned recruit died. Incorporating seedlings into the continuous dataset in this fashion allowed us to create IPMs using only one discrete stage.

We used data from the demographic study to estimate continuous vital rate functions describing survival, growth, probability of flowering, seed production, and recruit size. For each of these vital rates, we fit subpopulation-level models as well as models using data across all sites. We additionally fit models with and without density dependence, with and

without environmental covariates, and using data either from all years or from each unique annual transition. The basic model structure was the same for each vital rate (Table 2). All models included log-transformed leaf $size_t$ as a predictor. Log-transformed leaf $size_t$ squared was also included as a predictor if it decreased model AIC. Additional covariates indicating population size and environmental conditions were added to these basic models.

We modeled survival probability ($s(z)$) as a function of log-transformed leaf $size_t$ using generalized linear models with binomial error distributions. Flowering individuals were excluded from the data used to fit survival models, since *O. coloradensis* is a monocarpic perennial that nearly always dies after flowering. Probability of flowering ($Pb(z)$) was also modeled using generalized linear models with binomial error distributions, and was predicted by log-transformed leaf $size_t$ plus log-transformed leaf $size_t$ squared. We estimated seed production ($b(z)$) as a function of $size_t$ using negative binomial models because the count data was over-dispersed. We only used data from flowering plants in this analysis, and fit these models using the “glm.nb” function from the “MASS” R package (Venables & Ripley, 2002).

Plant $size_{t+1}$ ($G(z', z)$) was described as a series of Normal distributions with mean = μ_s and standard deviation = σ_s . Mean plant $size_{t+1}$ (μ_s) was modeled as a function of $size_t$ using linear models with Gaussian error. The standard deviation of plant $size_{t+1}$ (σ_s) was the residual standard error of these linear models, which we assumed to be constant. The distributions of recruit size in the next year ($c_o(z')$) were described by Normal distributions with the mean μ_r , and the standard deviation σ_r . μ_r and σ_r were the mean and standard deviation of observed plant size in the next year.

We estimated discrete vital rates for seeds using data from both greenhouse and field-based germination and seed viability studies. Previously-published data from a greenhouse

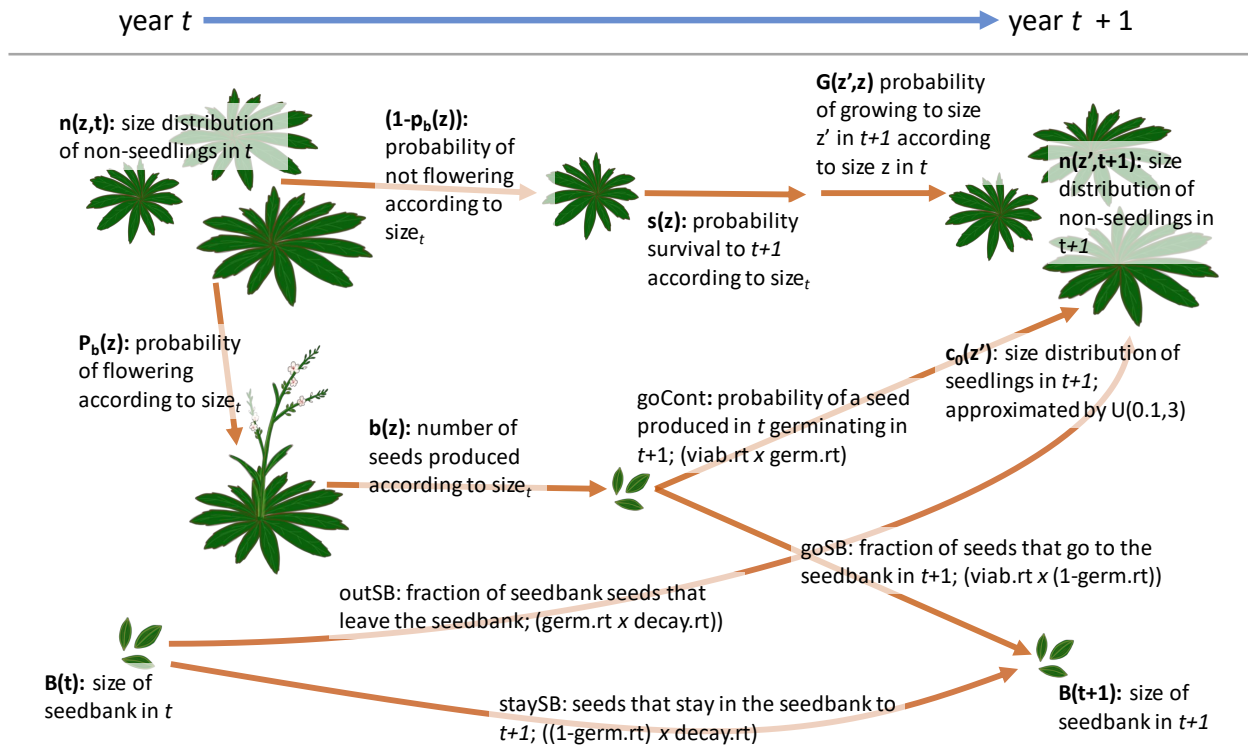


Figure 2: Diagram of the *O. coloradensis* life-cycle, with transitions labeled with the notation used in IPM equations. Based on model structures and notation from: (Paniw et al., 2017; Merow et al., 2014; Ellner et al., 2016). "germ.rt" = germination rate, "viab.rt" = viability rate, "decay.rt" = decay rate.

288 experiment using *O. coloradensis* seed capsules collected from the FEWAFB populations de-
 289 termined that viable seeds had an average germination rate of 20.3% after cold-stratification,
 290 and did not identify a consistent decline in germination rate over five years (Burgess et al.
 291 2005). This study also found that a seed capsule contained an average of 1.7 seeds, and that
 292 58.5% of seeds produced were viable. We conducted an additional seed study to determine
 293 if overwintering in natural conditions lead to a lower germination rate than was identified in
 294 the previous greenhouse study. We buried 60 field-collected seed capsules in mesh bags at 6
 295 locations near our demographic study plots at FEWAFB, and then recovered the seed bags
 296 after one winter. An average of 10% of seed capsules were not recoverable, likely because

297 they were non-viable and withered away or were eaten. We planted the recovered capsules in
298 standard greenhouse conditions, and found a mean germination rate of 6.8%. This germina-
299 tion rate was much lower than that identified by Burgess et al., however our seed study had
300 a much smaller sample size, reducing the reliability of our result. However, it is still likely
301 that true germination rates are much lower than those identified in greenhouse conditions, so
302 we reduced the germination rate identified by Burgess et al. by 20%. The following param-
303 eters we used to estimate the discrete seed vital rate parameters: viable seed germination
304 rate (germ. rate) = 0.16, viability rate of seeds produced by a parent plant (viab. rate) =
305 0.58, rate of natural seed death in the seedbank (death rate) = 0.10. We did not have the
306 data required to determine how these rates changed across subpopulations or in response to
307 abiotic variation, so we used the same seed vital rates for all IPM models (Table 2).

308 We used these vital rate functions and discrete parameters described above to construct
309 discretized IPM kernels. All kernels were numerically implemented using the “midpoint rule”
310 method (Easterling et al., 2000) with 500 bins, an upper size limit corresponding to 120% of
311 the maximum observed plant size and a lower size limit corresponding to 80% of the minimum
312 simulated seedling size of 0.1 cm. We then used eigen analysis of these kernels to estimate
313 the asymptotic population growth rate (λ), damping ratio, stable size distribution, and
314 reproductive value (Caswell, 2001; Ellner et al., 2016). We used 1000 iterations of bootstrap
315 re-sampling to estimate 95% bootstrap confidence intervals (95% CIs) for each continuous
316 vital rate parameter included in each IPM, as well as each estimate of λ (Merow et al., 2014;
317 Fieberg, Vitense, & Johnson, 2020). We were unable to estimate CIs for discrete seedbank
318 parameters because they were drawn from a previous publication. We used perturbation
319 analysis to determine the sensitivity and elasticity of λ to changes in germination rate,

320 viability rate, seed survival rate, and each parameter in each continuous vital rate model
321 (Morris & Doak, 2002). We used the IPM with all data and no density dependence or
322 environmental covariates (IPM “B”) for this analysis. All vital rate models and IPMs,
323 as well as the information derived from them, were used to evaluate the importance of
324 negative density dependence, demographic compensation, vital rate buffering, asynchronous
325 responses, and source-sink dynamics for persistence of *O. coloradensis* populations.

326 **Objective 2: Evaluating Persistence Mechanisms**

327 *Negative Density Dependence:* In order to determine the importance of density depen-
328 dence in *O. coloradensis* subpopulations, we compared subpopulation-level, all-transition
329 IPMs and vital rate functions that did and did not include population size in the current
330 year as a covariate in vital rate models (density-independent IPMs: “C”-“H” in Table 1;
331 density-dependent IPMs: “I”-“N”). We used AIC to identify significant differences be-
332 tween vital rate models with and without density dependence terms. We also used results
333 from subpopulation-level IPMs (Table 1: IPMs ”CC”-”NN”) for each transition to identify
334 relationships between subpopulation size in year t and $\ln(\lambda)$ (as in Fig. 1), as well as sub-
335 population size in year t and the ratio of population size in year $t+1$ and subpopulation size
336 in year t . In addition to population size information and $\ln(\lambda)$ values from our IPMs, we also
337 used population sizes and $\ln(\lambda)$ values from a previously-published demographic study of *O.*
338 *coloradensis* at the three FEWAFB subpopulations that we also monitored (Floyd & Ranker,
339 1998). A negative relationship between population size in year t and either $\ln(\lambda)$ or the ratio
340 of population size in year $t + 1$ to population size in year t would provide evidence for
341 negative density dependence. Additionally, significant differences between models with and

342 without population size predictor terms would constitute evidence for density dependence.

343 *Demographic Compensation:* To test for demographic compensation, we calculated the

344 correlation between environmental covariate coefficients in different vital rate models. A

345 negative correlation between coefficients of the same covariate in different vital rate models

346 indicated demographic compensation was taking place (Villellas et al., 2015; Dibner et al.,

347 2019). For example, if soil moisture had a positive effect on growth but a negative effect on

348 survival, this would be evidence for demographic compensation. For this correlation analysis

349 we used vital rate models that were fit using data from each subpopulation and both transi-

350 tions, and that included covariates for density dependence and all environmental covariates

351 (vital rate models from IPMs “S”-“X” in Table 1). We tested the significance of negative

352 correlations between environmental covariate coefficients using a randomization procedure

353 similar to that used by Villellas et al. (2015), where we randomly assigned an environmental

354 covariate coefficient drawn from the observed distribution of values for that coefficient to

355 each vital rate function, calculated a correlation matrix between those coefficients in each

356 vital rate function, and counted the number of negative correlations in that matrix. This

357 procedure was repeated 10,000 times to generate a null distribution of the expected number

358 of negative correlations between environmental coefficients that would occur randomly. We

359 compared the observed number of negative correlations between each environmental covari-

360 ate coefficient to these expected distributions of random correlations to determine statistical

361 significance. We could not test for demographic compensation in discrete seedbank vital rate

362 parameters because we did not know how they varied according to environmental conditions.

363 A significant negative correlation between environmental covariate coefficients in different

364 vital rate models would provide evidence for demographic compensation (Fig. 1).

365 *Vital Rate Buffering:* We tested for the presence of vital rate buffering in *O. coloradensis*

366 populations by comparing the variability of demographic rates to their importance. We used

367 an approach that scales both the standard deviation (variability metric) and sensitivity (im-

368 portance metric) of vital rates, allowing for a fair comparison of variability and importance

369 across vital rates with fundamentally different relationships between their mean and variance

370 (McDonald et al., 2017). Vital rates that are probabilities (i.e. survival, flowering, growth,

371 discrete seedbank transition probabilities, and seedling size) are constrained between zero

372 and one and thus typically have small variance as the mean approaches these limits, while

373 other vital rates are only constrained by zero and thus typically have variances that increase

374 as the mean increases (i.e. seed productivity) (Gaillard & Yoccoz, 2003). To enable a fair

375 comparison between these different categories of vital rates, we calculated the importance

376 and variability of probability and non-probability vital rates in different ways. The impor-

377 tance of probability vital rates was defined as the logit variance stabilized sensitivity, and the

378 variability was defined by the standard deviation of the logit transformed vital rate values

379 (McDonald et al., 2017; William A Link, Paul F Doherty, Fr., 2002). The importance of

380 non-probability vital rates was defined as the log-scaled sensitivity (or elasticity), and the

381 variability was defined by the standard deviation of the log-transformed vital rate values

382 (McDonald et al., 2017; Morris & Doak, 2002).

383 We used an IPM that was fit across all subpopulations using data from both transitions

384 (Table 1: IPM “B”) to calculate elasticity or logit VSS values for each discrete vital rate and

385 continuous vital rate function. We calculated the scaled standard deviation for each contin-

386 uous vital rate function using the vital rates that were fit uniquely for each subpopulation

387 and each transition (Table 1: IPMs “CC”-“NN”). Because we did not have site-level infor-

mation about discrete seedbank vital rates, we simulated both the maximum and minimum possible standard deviations for each discrete vital rate. We then proceeded with two comparisons of vital rate variability and importance, once using the maximum possible discrete vital rate standard deviation, and another using the minimum. In order to determine the correlation between a single importance/variability value pair for discrete vital rates and a string of value pairs for continuous vital rate functions, we calculated mean importance and variability values for each continuous vital rate function. A significant negative correlation between the mean or absolute scaled importance (logit VSS or elasticity) and mean or absolute variability (standard deviation of logit or log-transformed vital rates) across all vital rates would constitute support for the presence of vital rate buffering in this species (Fig. 1).

Asynchronous Responses and Source-Sink Dynamics: To determine whether *O. coloradensis* subpopulations showed asynchronous responses to environmental variation, we made a correlation matrix to determine how change in $\ln(\lambda)$ across each transition was correlated across each subpopulation, using values of $\ln(\lambda)$ derived from IPMs for each subpopulation (Table 1: IPMs “C”-“H”). We used the “mantel()” function from the “vegan” R package to perform a Mantel test, which determined if the Spearman correlation of $\ln(\lambda)$ across subpopulations was significantly related to the Euclidian distance between each subpopulation (Oksanen et al., 2020). A negative relationship between the distance between subpopulations and degree of correlation of $\ln(\lambda)$ would constitute evidence for spatial asynchrony between subpopulations (Fig. 1).

Because we did not have information about gene flow between subpopulations of *O. coloradensis* via pollination or seed dispersal, it was not possible to directly measure whether

411 fine-scale source-sink dynamics were acting in these populations. However, because variation
412 in population growth rate across space is a pre-requisite for source-sink dynamics, the pre-
413 viously described tests for spatial asynchrony in subpopulations can also provide evidence
414 for the existence of source-sink dynamics. Again, this would be a negative relationship of
415 distance between subpopulations and correlation of subpopulation $\ln(\lambda)$ (Fig. 1).

Table 2: Description of vital rates used in *O. coloradensis* IPMs

Vital Rate	Description	Model
$pEstab$	$P(\text{seed produced in } t \text{ establishes as a seedling in } t+1)$	$pEstab = \frac{\text{Num. new recruits in year } t+1}{\text{Num. seeds produced in year } t}$
$goCont$	$P(\text{seed produced in } t \text{ germinates in } t+1)$	$goCont = \text{viab. rate} \times \text{germ. rate}$
$outSB$	$P(\text{seedbank seed in } t \text{ germinates in } t+1)$	$outSB = \text{germ. rate} \times (1 - \text{death rate})$
$goSB$	$P(\text{seed produced in } t \text{ goes into the seedbank in } t+1)$	$goSB = \text{viab. rate} \times (1 - \text{germ. rate})$
$staySB$	$P(\text{seedbank seed in } t \text{ stays in the seedbank in } t+1)$	$staySB = (1 - \text{germ. rate}) \times (1 - \text{death rate})$
$Survival(s(z))$	$P(\text{survival from } t \text{ to } t+1)$	$\text{logit}(\text{survival}) \sim \beta_0 + \beta_1(\ln(\text{size}_t)) + \epsilon$
$Flowering(Pb(z))$	$P(\text{flowering in } t)$	$\text{logit}(\text{flowering}) \sim \beta_0 + \beta_1(\ln(\text{size}_t)) + \beta_2(\ln(\text{size}_t)^2) + \epsilon$
$Seed \ prod.(b(z))$	$\text{Seed production in } t$	$\exp(\text{seed number}) \sim \beta_0 + \beta_1(\ln(\text{size}_t)) + \epsilon$
$Growth(G(z', z))$	$\text{Distribution of plant size in year } t$	$G(z', z) = N(\mu_s, \sigma_s);$ $\mu_s \sim \beta_0 + \beta_1(\ln(\text{size}_t)) + \epsilon;$ $\sigma_s \sim RSE(\beta_0 + \beta_1(\ln(\text{size}_t)) + \epsilon)$
$Recruit \ size(c_o(z'))$	$\text{Distribution of new recruit size in year } t$	$c_o(z') = N(\mu_r, \sigma_r);$ $\mu_r = \text{mean}(\text{size of recruits in } t);$ $\sigma_r = \text{stnd. dev. (size of recruits in } t)$

* RSE = residual standard error

416 Results**417 Vital Rate Models**

418 In vital rate models parameterized for each population using data from both transitions,

419 we found that larger non-reproductive plants are more likely to survive to year $t+1$ than

420 smaller plants (Fig. 3A). Plants below 7.5 cm in year t are likely to become larger in year

421 $t+1$, while plants larger than 7.5 cm are likely to become smaller in the next year (Fig. 3 B).

422 Flowering probability is best approximated as a quadratic polynomial: flowering probability

423 rises when $\ln(\text{size}_t)$ approaches 2.5 (12 cm), but plants with the largest leaves exhibit low

424 flowering probability (Fig. 3 C). The number of seeds that a reproductive plant produces

425 increases sharply with $\ln(\text{size}_t)$ (Fig. 3 D). The inclusion of additional covariates did not

426 alter the overall shape or sign of the relationships between $\ln(\text{size}_t)$ and vital rates, so models

427 shown in Figure 3 did not include any additional covariates beyond $\ln(\text{size}_t)$.

428 Objective 1: Quantifying the Importance of the Seedbank Stage

429 *Integral Projection Models:* We found that including a discrete seedbank stage in IPMs

430 for *O. coloradensis* significantly increased the asymptotic population growth rate. The con-

431 tinuous state-only IPM (Table 1: IPM “A”) predicted an asymptotic $\ln(\lambda)$ of 0.27 for all

432 populations (95% CI: 0.269 - 0.271), while the continuous + discrete state IPM (Table 1:

433 IPM “B”) predicted an asymptotic $\ln(\lambda)$ of 0.65 (populations (95% CI: 0.648 - 0.650). All

434 subsequent IPM results refer to models that included a discrete seedbank state.

435 The simplest two-state IPMs that excluded density dependence and environmental vari-

436 ation indicated that both the Soapstone prairie and FEWAFB populations had positive

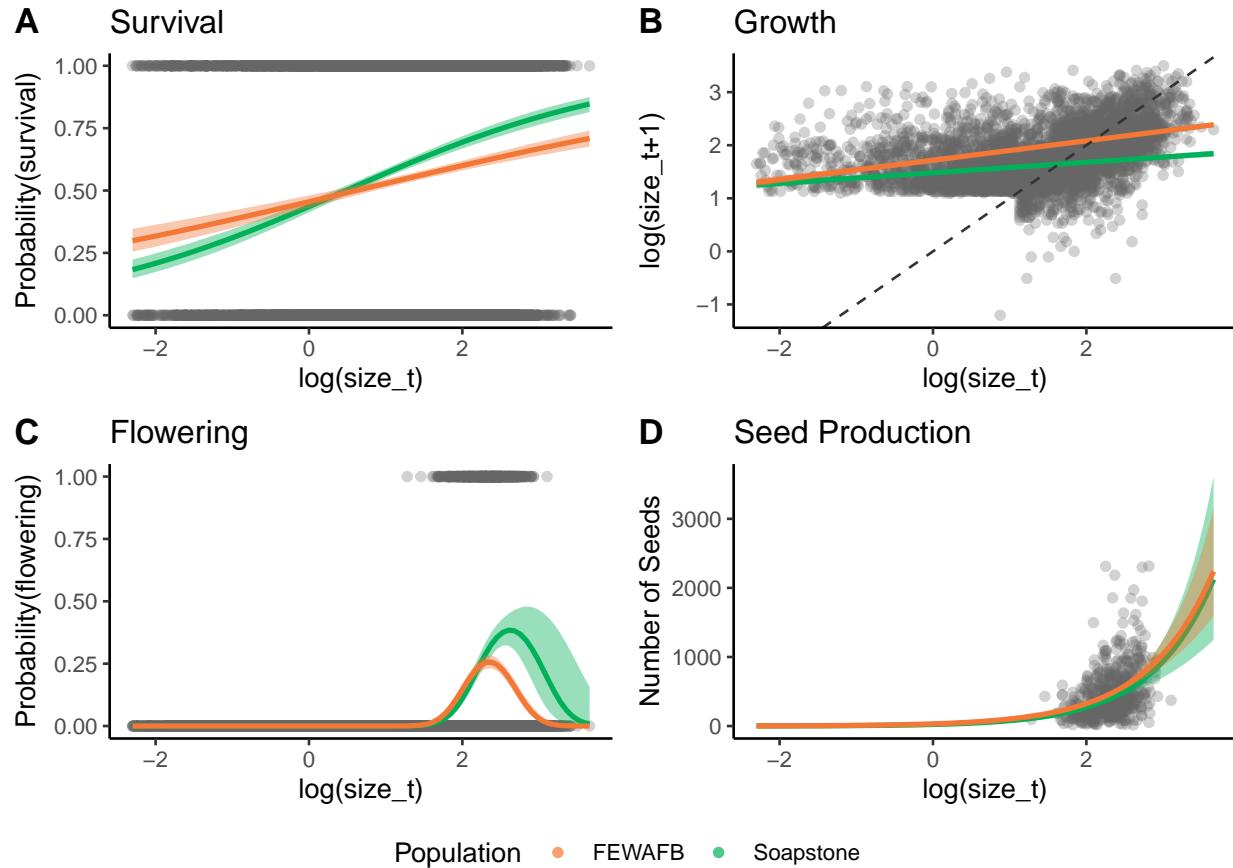


Figure 3: The effect of current year size ($\ln(\text{size}_t)$) on vital rates in monitored *O. coloradensis* populations. Data for all sites and all transitions is shown. Lines indicate vital rate functions for each population, and include only $\ln(\text{size}_t)$ as a predictor, with the exception of flowering models, which include a $(\ln(\text{size}_t))^2$ term. Bands around each line show 95% confidence intervals. The dashed line in panel **B** shows a 1:1 line. The sharp cut-off in $\ln(\text{size}_{t+1})$ in panel **B** is due to the fact that two-year-old plants could not be seedlings, which were classified as any plant less than 3 cm in size.

437 population growth rates (Table 1: Soapstone prairie- IPM “AA”, $\ln(\lambda) = 0.50$; FEWAFB –
 438 IPM “BB”, $\ln(\lambda) = 0.73$). The Diamond Creek subpopulation at FEWAFB had the highest
 439 population growth rate from 2018 to 2020 (Table 1: IPM “D”, $\ln(\lambda) = 0.113$), while the
 440 HQ3 subpopulation at Soapstone prairie had the lowest growth rate (Table 1: IPM “G”,
 441 $\ln(\lambda) = 0.395$). We parameterized multiple other sets of IPMs that used different combina-
 442 tions of covariates in their vital rate models, and almost all identified a positive population

443 growth rate (Table 1).

444 A density-independent, discretized IPM kernel (made using IPM “B” in Table 1) shows
445 transition probabilities within and between the discrete and continuous stages of the *O.*
446 *coloradensis* lifecycle when all populations and transitions are considered together (Fig. 4
447 A). Relative to the rest of the kernel, there is a very high probability that seeds stay in the
448 seedbank, as well as a large contribution of seeds from medium-sized adult plants to the
449 seedbank in the next year. The rates at which seeds are produced by adult plants and stay
450 in the seedbank have the most impact on population growth rate (Fig. 4 C).

451 **Objective 2: Evaluating Persistence Mechanisms**

452 *Negative Density Dependence:* There is moderate evidence that negative density-dependence
453 is acting to maintain populations of *O. coloradensis*. AIC comparison of continuous vital
454 rate models indicate that density-dependent models are better predictors of the majority
455 of vital rates than density-independent models in most subpopulations (Table 3). Models
456 that included population size in the previous year as a covariate were better predictors of
457 growth in five of six subpopulations. Density dependent models were better predictors of
458 survival and seed production than density independent models in four out of six subpopula-
459 tions, and density dependent models of flowering were better in one subpopulation. Recruit
460 size distribution was not affected by density dependence—AIC model comparison did not
461 indicate substantial differences, either negative or positive, between recruit size models with
462 and without density dependence terms in any subpopulation. The vital rate models for the
463 Meadow population at Soapstone Prairie were least affected by density dependence. Al-
464 though density dependence is important for *O. coloradensis* in many situations, it appears

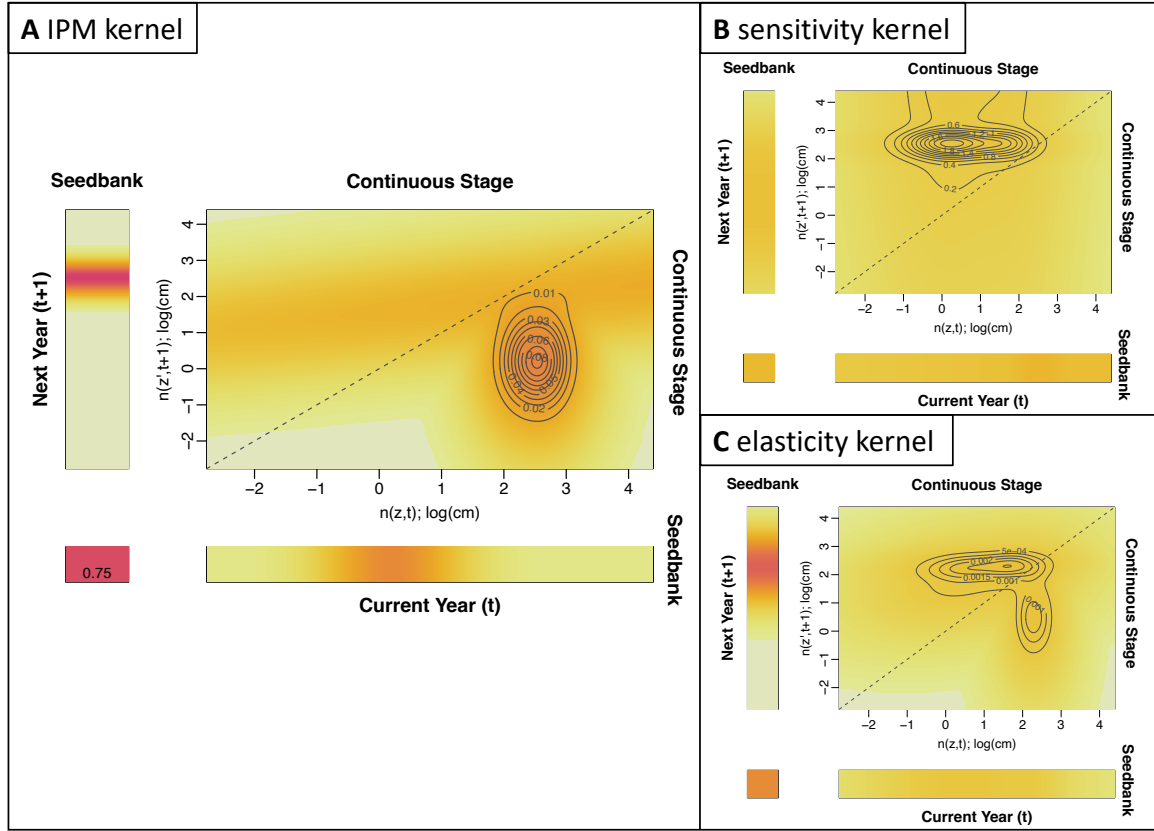


Figure 4: Visualizations of the *O. coloradensis* IPM kernels. **A** The IPM kernel for *O. coloradensis*. This kernel shows a density-independent IPM constructed using all data from all transitions (IPM "B"). **B** Sensitivity of the IPM kernel. **C** Elasticity of the IPM kernel. In all panels, color indicates probability, with darker colors corresponding to higher probability, and lighter colors corresponding to lower probability. The dashed line shows a 1:1 line.

only to be acting to decrease lambda at high density (as in the highly dense Diamond Creek or HQ5 subpopulations), but not clearly increasing lambda at low density (as in the sparsely populated Meadow subpopulation). We also found that population growth rate is generally higher when population size is smaller, but only when comparing the relationship between $\ln(\lambda)$ and population size within a subpopulation (Fig. 5 A and C). There is also a negative relationship within each subpopulation between population size in year t and the ratio of subpopulation size in $t+1$ to subpopulation size in t (Fig. 5 B and D). However, when

- ⁴⁷² looking across all subpopulations, there is not a clear relationship between subpopulation
⁴⁷³ size in t and either $\ln(\lambda)$ or the ratio of subpopulation size in $t+1$.

Table 3: Comparison of vital rate models that do and do not include density dependence. The “DI” and “DD” rows contain AIC values for each vital rate model in each subpopulation for models that are density-independent (DI) and density-dependent (DD). The difference between the AIC of DI and DD models is shown in the ΔAIC column. Bold text indicates that the $|\Delta\text{AIC}|$ value is > 3 , which means that including a term for density dependence substantially changed that vital rate model. A positive $|\Delta\text{AIC}|$ indicates that including density dependence improved the model, while a negative value indicates that including density dependence made model fit worse.

Vital Rate Model		Subpopulation					
		Crow Creek	Diamond Creek	Unnamed Creek	HQ5	HQ3	Meadow
Survival	DI	776.58	1012.68	2684.34	3242.63	716.66	166.13
	DD	757.84	905.39	26848.74	2922.91	637.84	166.83
	ΔAIC	18.74	107.28	-0.41	320.33	78.82	-0.70
Growth	DI	510.34	953.29	1098.95	1570.93	300.18	116.54
	DD	506.61	931.15	1068.14	1112.78	269.73	113.88
	ΔAIC	3.73	22.15	30.811	458.15	30.45	2.66
Flowering	DI	371.68	523.30	1087.93	538.52	191.46	104.24
	DD	373.31	523.74	1087.48	483.99	193.22	106.96
	ΔAIC	-1.63	-0.44	0.45	54.52	-1.76	-1.72
Seed production	DI	842.00	1580.85	2815.89	1423.02	598.75	280.09
	DD	835.59	1566.83	2817.19	1419.32	594.63	281.45
	ΔAIC	6.41	14.02	-1.29	3.71	4.12	-1.35
Recruit size	DI	921.31	1028.23	3378.43	4629.87	967.83	173.03
	DD	923.24	1026.63	3380.53	4631.84	969.06	175.02
	ΔAIC	-1.93	1.61	-1.93	-1.97	-1.23	-1.99

- ⁴⁷⁴ *Demographic Compensation:* Our analyses did not identify signatures of demographic
⁴⁷⁵ compensation in *O. coloradensis* populations. While there were negative correlations between
⁴⁷⁶ the effect of mean growing season temperature on vital rates for five combinations of vital
⁴⁷⁷ rates, none of these correlations were significant (Table 4). The only significant correlation

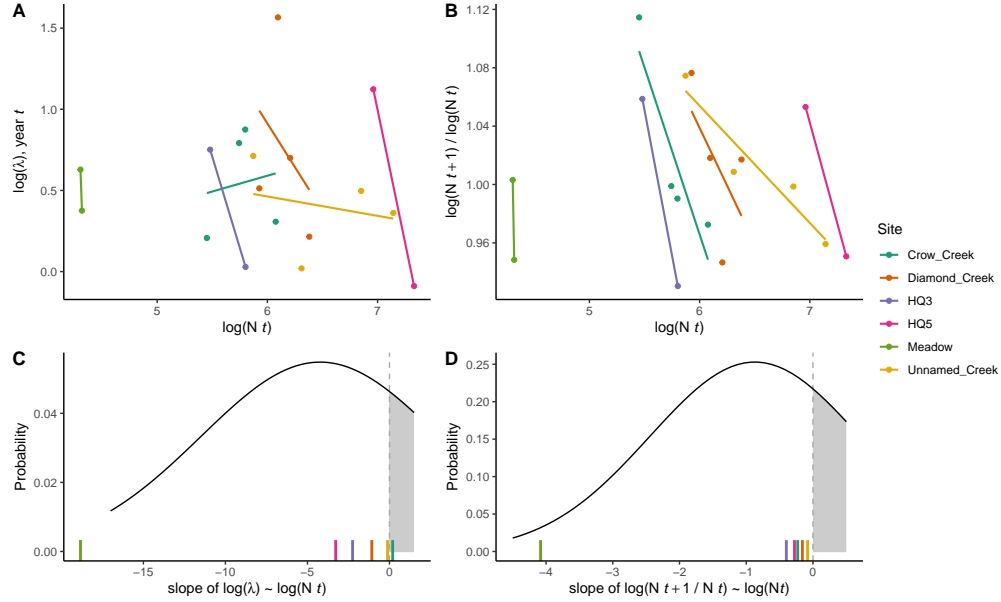


Figure 5: **A** Within the same subpopulation, population growth rate ($\ln(\lambda)$) calculated from IPMs decreases as population size increases. **B** Population growth rate calculated by change in population size from year t to year $t+1$ also decreases as population size increases in the same subpopulation. In **A** and **B**, each point represents values calculated from data from one transition in one subpopulation. Lines show linear regressions of the relationships between $\ln(N_t)$ and the respective response variable in each subpopulation. Rug plots in panels **C** and **D** show the slope of each regression line in panels **A** and **B**, respectively. The normal distributions in **C** and **D** were created using the means and standard deviations of these slopes. According to these distributions of observed slopes, there is a 28% probability that the true relationship between $\ln(\lambda)$ and $\ln(N_t)$ is positive, and a 29% probability that the true relationship between $\ln(N_t)$ and $\ln(N_{t+1}/N_t)$ is positive. In all panels, “N” indicates the number of individuals in a subpopulation.

478 was positive. Ten thousand correlations of randomly assigned coefficients found that the
 479 number of negative correlations in a matrix can be described by a normal distribution with
 480 a mean of 4.97 and a standard deviation of 1.60. Using this distribution as a null model,
 481 there was a 50.7% probability of observing five negative correlations. Although there is
 482 no significant evidence for demographic compensation, it is notable that the effect of mean
 483 growing season temperature on distribution of recruit size was negatively correlated with the
 484 effect of growing season temperature on all other vital rates. We were only able to compare

⁴⁸⁵ coefficients across vital rate models for mean growing season temperature, because including
⁴⁸⁶ precipitation and mean winter temperature as covariates resulted in overfitting in some cases.

Table 4: Pearson correlations between mean growing season temperature coefficients in each continuous vital rate function. Below each correlation value is the *P* value for that correlation. Bold text indicates a significant correlation.

		Vital Rate				
		<i>Flowering</i>	<i>Survival</i>	<i>Growth</i>	<i>Seed</i>	<i>Recruit</i>
Vital Rate	<i>Flowering</i>	1.00	0.474	0.136	-0.073	-0.786
		(0)	(0.342)	(0.797)	(0.890)	(0.064)
	<i>Survival</i>	1.00	0.886	0.675	-0.3570	
		(0)	(0.019)	(0.141)	(0.237)	
	<i>Growth</i>	1.00	0.664	-0.270		
		(0)	(0.150)	(0.606)		
	<i>Seed Prod.</i>	1.00	-0.432			
		(0)	(0.393)			
	<i>Recruit Size</i>	1.00				
		(0)				

⁴⁸⁷ *Vital Rate Buffering:* We did not identify strong evidence of vital rate buffering in the
⁴⁸⁸ *O. coloradensis* populations we observed. Vital rate importance (either logistic VSS or elas-
⁴⁸⁹ ticity) and variability (corrected SD) were not significantly negatively correlated, regardless
⁴⁹⁰ of the simulated standard deviation for discrete vital rates we used (Fig. 6; correlation with
⁴⁹¹ minimum discrete vital rate SD (**A**): $r = 0.43$, $P = 0.25$; correlation with maximum dis-
⁴⁹² crete vital rate SD (**B**): $r = -0.07$, $P = 0.85$). As a vital rate became more important for
⁴⁹³ determining population growth rate, it did not become significantly less variable, showing
⁴⁹⁴ no evidence that vital rate buffering is taking place (Fig. 1).

⁴⁹⁵ *Asynchronous Responses and Source-Sink Dynamics:* We did not identify a signature of
⁴⁹⁶ asynchronous responses to environmental variation in *O. coloradensis* populations. There

497 was not a significant relationship between the Spearman correlation of $\ln(\lambda)$ between subpop-
498 ulations and their spatial proximity (Mantel statistic = 0.396, $P = 0.06$). We also performed
499 Mantel tests using $\ln(\lambda)$ correlation and distance matrices calculated uniquely for each pop-
500 ulation. There was not a significant relationship between subpopulation growth rate and
501 spatial proximity at either Soapstone prairie (Mantel statistic = -0.659, $P = 0.83$) or FE-
502 WAFB (Mantel statistic = 0.798, $P = 0.33$). While these tests did not identify significant
503 relationships, we did find a positive relationship between correlation of $\ln(\lambda)$ and distance
504 between subpopulations at Soapstone prairie, and a negative relationship between subpopu-
505 lations at FEWAFB. Collectively, these results fail to provide support for both asynchronous
506 responses and fine-scale source-sink dynamics in these *O. coloradensis* populations.

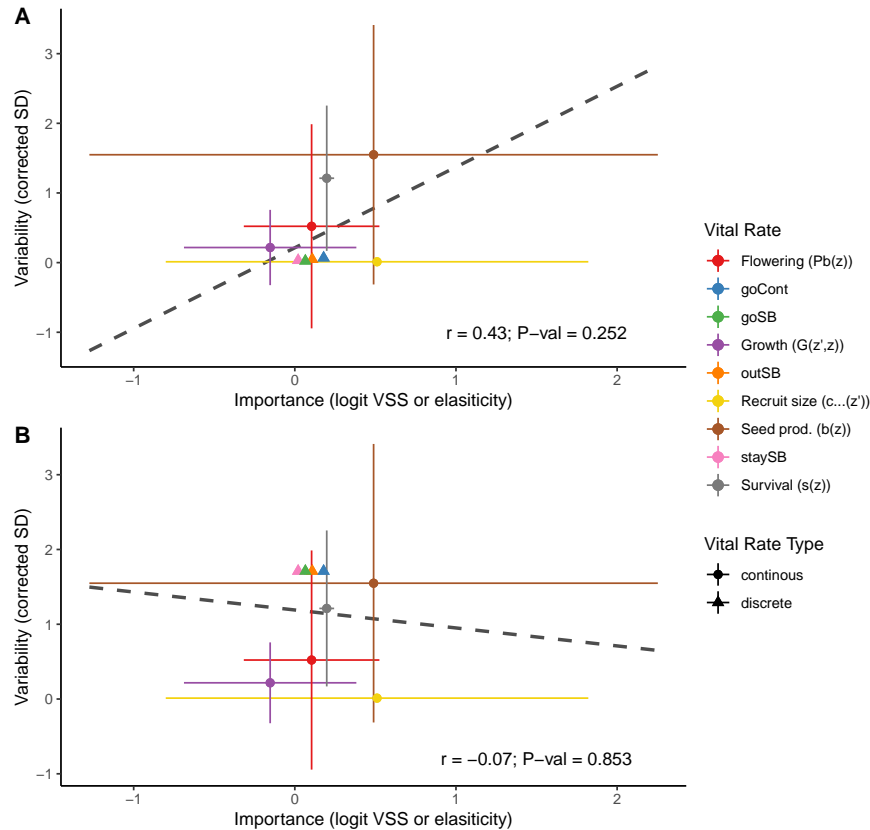


Figure 6: The relationship between the variability of each vital rate (measured by corrected standard deviation) and its importance (measured by logit VSS or elasticity) does not show support for vital rate buffering. In these figures, a triangle indicates importance and variability for a discrete vital rate parameter, while a circle indicates the mean of importance and variability across an entire continuous vital rate function. Error bars around continuous vital rate means span the the 5th to 95th percentiles of either importance or variability values calculated for an entire continuous vital rate function. Dashed lines show the correlation between (mean) variability and (mean) importance across all vital rates. Because we lacked data to calculate the actual standard deviation of discrete vital rates, we simulated both the minimum and maximum possible standard deviation for each of these rates. (A) With the minimum possible discrete vital rate variability, there is a positive but insignificant correlation between vital rate variability and importance ($r = 0.43, P = 0.25$). (B) Using the maximum possible discrete vital rate variability, there is a negative but insignificant correlation between vital rate variability and importance ($r = -0.07, P = 0.85$).

507 **Discussion**

508 Our demographic analysis of the two largest known populations of the globally rare
509 *Oenothera coloradensis* evaluated the importance of seedbanks to population dynamics and
510 identified the demographic mechanisms that allow this rare species to persist. First, we found
511 that including information about cryptic life stages alters the outcomes of the population
512 model (Paniw et al., 2017; Nguyen et al., 2019). *O. coloradensis* populations show signs
513 of negative density-dependence at the subpopulation scale (Fig. 5; Table 3). However,
514 these populations do not show substantial evidence of demographic compensation, vital rate
515 buffering, spatial asynchrony, or fine-scale source-sink dynamics. This may indicate that
516 while these mechanisms may be important for the persistence of many small populations of
517 rare plants, they are not strictly necessary in all cases.

518 Including a discrete seedbank state in an IPM increased the asymptotic population growth
519 rate compared to an IPM with only a continuous, size-based state, although both growth
520 rates were still positive (Table 1: with seedbank: IPM “B”, $\ln(\lambda) = 0.65$; without seedbank:
521 IPM “A”, $\ln(\lambda) = 0.27$). The importance of the including the seedbank in the model aligned
522 with our expectations, and also align with the conventional notion that seedbanks can act as
523 buffers against stochastic causes of population decline. The discrete rates for the probability
524 of persisting and transitioning out of the seedbank have high elasticity in the IPMs in which
525 they are included, but not the highest elasticity of any vital rate (Fig. 4 C). The rate at
526 which seeds produced by adult plants in year t go into the seedbank in year $t+1$ is the vital
527 rate function with highest elasticity. Previous matrix population models of *O. coloradensis*
528 without a seedbank state that were constructed in the 1990s identified the emergence rate

of new seedlings as the vital rate most important for determining $\ln(\lambda)$ (Floyd & Ranker, 1998). Our finding that seedbank state transitions are important for this species aligns with this previous result, since rate of seedling emergence is the above-ground plant vital rate that is closest to the seedbank in this plant's life cycle. An important caveat to our comparison of models with and without seedbank stages is the fact that the seedbank vital rate parameters we used were inferred from laboratory tests of germination and viability rates, which may be imperfect representations of *in-situ* rates of viability and germination. The annual rate of seed death (10%) was inferred from an *in-situ* study, but is likely imprecise because of low sample size. Regardless of these potential sources of error, our results reinforce the fact that the seedbank can be an important element of a perennial plant's lifecycle, and if possible, should be modeled explicitly based on *in-situ* estimates of the probability of seeds going into, persisting in, and emerging from the seedbank.

We found evidence that, of the five proposed demographic mechanisms of small population persistence, negative density dependence was the only one acting in these *O. coloradensis* populations. Including population size in the previous year as a covariate in vital rate models typically improved model fit, suggesting that density dependence is an important driver of growth, survival, and reproduction (Table 3). Within a single subpopulation, population growth rate and the ratio of population size in year $t+1$ to year t was generally higher when population size in year t was smaller (Fig. 5), which indicates that negative density dependence prevents subpopulations from crashing when their population size is very small. However, this pattern of higher growth rate at low population sizes did not exist when considering all subpopulations together (Fig. 5). This could indicate that each subpopulation is close to its carrying capacity for *O. coloradensis*. This may indicate that the number

of individuals is close to carrying capacity in each subpopulation, and that growth rate increases when the population size in a given subpopulation is small in comparison to its subpopulation-specific carrying capacity. *O. coloradensis* vital rates had correlated responses to variation in the abiotic environment (Table 4), which is the inverse of what is expected if demographic buffering is taking place. It is possible that a signal of demographic buffering would appear if we considered different abiotic variables such as disturbance frequency, or had more data. Vital rate buffering also was not identified, either with the minimum or maximum possible simulated discrete vital rate variability (Fig. 6). Vital rates with higher variability (higher SD) did not have a significantly higher or lower importance for determining $\ln(\lambda)$ in comparison to less variable vital rates. This indicates that vital rate buffering is not stabilizing $\ln(\lambda)$ after abiotic or demographic perturbation. The evidence for spatial asynchrony and fine-scale source-sink dynamics was also not strong. Mantel tests did not identify a significant relationship between the correlation of $\ln(\lambda)$ between subpopulations and their spatial proximity, but did identify non-significant relationships between $\ln(\lambda)$ correlation and proximity. However, this relationship was positive in Soapstone prairie subpopulations and negative in FEWAFF subpopulations, which provides inconsistent support for these mechanisms.

It is somewhat surprising that negative density dependence is the only mechanism of small population persistence that has significant support in *O. coloradensis* populations, since multiple mechanisms have been identified in other rare species (Dibner et al., 2019). It is possible that support for one or more of these persistence mechanisms could emerge if more information about abiotic variation across space and time and data from more annual transitions was available for analysis. One potential explanation is that, while this species is a

globally rare endemic with isolated subpopulations, it often grows at high local density. This strategy, which Rabinowitz describes as “locally abundant in a specific habitat but restricted geographically,” may allow *O. coloradensis* to bypass the problems that small populations typically face, such as genetic and demographic bottlenecks that make them susceptible to stochastic environmental variation (Rabinowitz, 1981). It has also been shown that rare species are more likely than common species to benefit from facilitative interspecific interactions (Calatayud et al., 2020). *O. coloradensis* may participate in facilitative interactions with other species that increase its probability of persistence, although determining this will require further, community-level analysis. Our results imply that not all rare species can be treated equally. While demographic strategies that help maintain persistence may be effective for some species, other species may employ different strategies. This further emphasizes the importance of carefully considering the specific population and its community dynamics when managing and conserving rare species.

Our analysis of the population dynamics of *Oenothera coloradensis* at two distinct locations shows that this species has a lifecycle that is strongly influenced by introduction and persistence of seeds into a seedbank. More broadly, we show that this rare endemic species shows signs of negative density dependence. Populations of *O. coloradensis* may additionally be maintained via high local abundances that allow them to escape the challenges of small population size that rare species often face (Rabinowitz, 1981). These findings reinforce the importance of careful evaluation of the unique population dynamics of rare species to inform successful conservation and management.

Author Contributions: AES, DCL, and BH contributed to study conception and design and collected demographic data. Analysis was performed by AES with contributions from DCL, MP

598 and RSG. AES wrote the manuscript with contributions from all authors.

599 **Data Availability Statement:** All data that has not previously been published will be
600 available from Dryad. All code will be available to download from a public GitHub repository.

601 **References**

- 602 Abbott, R. E., Doak, D. F., & Peterson, M. L. (2017). Portfolio effects, climate change,
603 and the persistence of small populations: analyses on the rare plant *Saussurea weberi*.
604 *Ecology*, 98(4), 1071–1081. <https://doi.org/10.1002/ecy.1738>
- 605 Arnoldi, J. F., Loreau, M., & Haegeman, B. (2019). The inherent multidimensionality of
606 temporal variability: how common and rare species shape stability patterns. *Ecology*
607 Letters, 22(10), 1557–1567. <https://doi.org/10.1111/ele.13345>
- 608 Burgess, L. M. (2003). *Impacts of Mowing, Burning, and Climate on Germination and*
609 *Seedling Recruitment of Colorado Butterfly Plant (Gaura neomexicana ssp. coloradensis)* (Unpublished doctoral dissertation). University of Wyoming.
- 610 Burgess, L. M., Hild, A. L., & Shaw, N. L. (2005). Capsule treatments to enhance seedling
611 emergence of *Gaura neomexicana* ssp. *coloradensis*. *Restoration Ecology*, 13(1), 8–14.
612 <https://doi.org/10.1111/j.1526-100X.2005.00002.x>
- 613 Burner, R. C., Drag, L., Stephan, J. G., Birkemoe, T., Wetherbee, R., Muller, J., Siitonens, J.,
614 Snäll, T., Skarpaas, O., Potterf, M., Doerfler, I., Gossner, M. M., Schall, P., Weisser,
615 W. W., & Sverdrup-Thygeson, A. (2022). Functional structure of European forest
616 beetle communities is enhanced by rare species. *Biological Conservation*, 267(June
617 2021). <https://doi.org/10.1016/j.biocon.2022.109491>
- 618 Calatayud, J., Andivia, E., Escudero, A., Melián, C. J., Bernardo-Madrid, R., Stof-
619 fel, M., Aponte, C., Medina, N. G., Molina-Venegas, R., Arnan, X., Rosvall,
620 M., Neuman, M., Noriega, J. A., Alves-Martins, F., Draper, I., Luzuriaga, A.,
621 Ballesteros-Cánovas, J. A., Morales-Molino, C., Ferrandis, P., ... Madrigal-González,
622 J. (2020). Positive associations among rare species and their persistence in eco-
623 logical assemblages. *Nature Ecology and Evolution*, 4(1), 40–45. Retrieved from
624

- 625 <http://dx.doi.org/10.1038/s41559-019-1053-5> <https://doi.org/10.1038/s41559-019-1053-5>
- 626
- 627 Caswell, H. (2001). *Matrix Population Models: Construction, Analysis, and Interpretation* (2nd ed.). Sinauer Associates.
- 628
- 629 Dibner, R. R., Peterson, M. L., Louthan, A. M., & Doak, D. F. (2019). Multiple mechanisms 630 confer stability to isolated populations of a rare endemic plant. *Ecological Monographs*, 631 89(2), 1–16. <https://doi.org/10.1002/ecm.1360>
- 632 Drury, W. H. (1974). Rare species. *Biological Conservation*, 6(3), 162–169. [https://doi.org/10.1016/0006-3207\(74\)90061-5](https://doi.org/10.1016/0006-3207(74)90061-5)
- 633
- 634 Easterling, M. R., Ellner, S. P., & Dixon, P. M. (2000). Size-Specific Sensitivity: Applying 635 a New Structured Population Model. *Ecology*, 81(3), 694–708. [https://doi.org/10.1890/0012-9658\(2000\)081\[0694:SSSAAN\]2.0.CO;2](https://doi.org/10.1890/0012-9658(2000)081[0694:SSSAAN]2.0.CO;2)
- 636
- 637 Ellner, S. P., Childs, D. Z., & Rees, M. (2016). *Data-driven Modelling of Structured 638 Populations*. Switzerland: Springer International Publishing. Retrieved 639 from <http://link.springer.com/10.1007/978-3-319-28893-2> <https://doi.org/10.1007/978-3-319-28893-2>
- 640
- 641 Ellner, S. P., & Rees, M. (2006). Integral projection models for species with complex 642 demography. *American Naturalist*, 167(3), 410–428. <https://doi.org/10.1086/499438>
- 643 Enquist, B. J., Feng, X., Boyle, B., Maitner, B., Newman, E. A., Jørgensen, P. M., 644 Roehrdanz, P. R., Thiers, B. M., Burger, J. R., Corlett, R. T., Couvreur, T. L., 645 Dauby, G., Donoghue, J. C., Foden, W., Lovett, J. C., Marquet, P. A., Merow, C., 646 Midgley, G., Morueta-Holme, N., ... McGill, B. J. (2019). The commonness of rarity: 647 Global and future distribution of rarity across land plants. *Science Advances*, 5(11), 648 1–14. <https://doi.org/10.1126/sciadv.aaz0414>
- 649 Fieberg, J. R., Vitense, K., & Johnson, D. H. (2020). Resampling-based methods for 650 biologists. *PeerJ*, 2020(3). <https://doi.org/10.7717/peerj.9089>
- 651 Floyd, S. K., & Ranker, T. A. (1998). Analysis of a Transition Matrix Model for *Gaura* 652 neomexicana Ssp . *coloradensis* (Onagraceae) Reveals Spatial and Temporal Demo- 653 graphic Variability. *International Journal of Plant Sciences*, 159(5), 853–863.
- 654 Gaillard, J.-M., & Yoccoz, N. G. (2003, December). Temporal variation in survival of

- 655 mammals: A case of environmental canalization? *Ecology*, 84(12), 3294–3306.
- 656 Heidel, B., Tuthill, D., & Wallace, Z. (2021). *33-Year Population Trends of Colorado*
657 *Butterfly Plant (Oenothera Coloradensis; Onagraceae), a Short-Lived Riparian Species*
658 *on F. E. Warren Air Force Base, Laramie County, Wyoming* (Tech. Rep.). Laramie,
659 WY: Prepared for U.S. Fish and Wildlife Service and F. E. Warren Air Force Base by
660 the Wyoming Natural Diversity Database (University).
- 661 Hilde, C. H., Gamelon, M., Sæther, B. E., Gaillard, J. M., Yoccoz, N. G.,
662 & Pélabon, C. (2020). The Demographic Buffering Hypothesis: Evidence and Challenges. *Trends in Ecology and Evolution*, xx(xx). Retrieved from <https://doi.org/10.1016/j.tree.2020.02.004> <https://doi.org/10.1016/j.tree.2020.02.004>
- 663 Jennings, M. (2000). Endangered and Threatened Wildlife and Plants: Threatened Status for
664 the Colorado Butterfly Plant (*Gaura neomexicana* ssp. *coloradensis*) From Southeastern Wyoming, Northcentral Colorado, and Extreme Western Nebraska. *Federal Register: The Daily Journal of the United States*, 65(202), 62302–62310. [https://doi.org/10.1016/0196-335x\(80\)90058-8](https://doi.org/10.1016/0196-335x(80)90058-8)
- 665 Jongejans, E., Sheppard, A. W., & Shea, K. (2006). What controls the population dynamics
666 of the invasive thistle *Carduus nutans* in its native range? *Journal of Applied Ecology*,
667 43(5), 877–886. <https://doi.org/10.1111/j.1365-2664.2006.01228.x>
- 668 Kauffman, M. J., Pollock, J. F., & Walton, B. (2004). Spatial structure, dispersal, and
669 management of a recovering raptor population. *American Naturalist*, 164(5), 582–597.
670 <https://doi.org/10.1086/424763>
- 671 Leitão, R. P., Zuanon, J., Villéger, S., Williams, S. E., Baraloto, C., Fortune, C., Mendonça,
672 F. P., & Mouillot, D. (2016). Rare species contribute disproportionately to the functional
673 structure of species assemblages. *Proceedings of the Royal Society B: Biological Sciences*, 283(1828). <https://doi.org/10.1098/rspb.2016.0084>
- 674 Levins, R., & Culver, D. (1971). Regional Coexistence of Species and Competition between
675 Rare Species. *Proceedings of the National Academy of Sciences*, 68(6), 1246–1248.
676 <https://doi.org/10.1073/pnas.68.6.1246>
- 677 Lyons, K. G., Brigham, C. A., Traut, B. H., & Schwartz, M. W. (2005). Rare species

- 685 and ecosystem functioning. *Conservation Biology*, 19(4), 1019–1024. <https://doi.org/10.1111/j.1523-1739.2005.00106.x>
- 686
- 687 Magurran, A. E., & Henderson, P. A. (2011). Commonness and Rarity. In A. E. Magurran
688 & B. J. McGill (Eds.), *Biological diversity : frontiers in measurement and assess-*
689 *ment* (pp. 97–104). Oxford; New York: Oxford University Press. Retrieved from
690 <https://www.researchgate.net/publication/281461811>
- 691 May, R. M. (1973). Stability in Randomly Fluctuating Versus Deterministic Environments.
692 *The American Naturalist*, 107(957), 621–650.
- 693 McDonald, J. L., Franco, M., Townley, S., Ezard, T. H., Jelbert, K., & Hodgson, D. J.
694 (2017). Divergent demographic strategies of plants in variable environments. *Nature
695 Ecology and Evolution*, 1(2). <https://doi.org/10.1038/s41559-016-0029>
- 696 Merow, C., Dahlgren, J. P., Metcalf, C. J. E., Childs, D. Z., Evans, M. E., Jongejans, E.,
697 Record, S., Rees, M., Salguero-Gómez, R., & McMahon, S. M. (2014). Advancing
698 population ecology with integral projection models: A practical guide. *Methods in
699 Ecology and Evolution*, 5(2), 99–110. <https://doi.org/10.1111/2041-210X.12146>
- 700 Morris, W. F., & Doak, D. F. (2002). *Quantitative Conservation Biology: Theory and
701 Practice of Population Viability Analysis*. Sunderland, MA: Sinauer Associates.
- 702 Munk, L. M. (1999). *Colorado butterfly plant (Gaura neomexicana spp. col-*
703 *oradensis) regeneration with removal of Canada thistle (Cirsium arvense) or na-*
704 *tive herbs* (Doctoral dissertation, University of Wyoming). Retrieved from
705 <http://dx.doi.org/10.1016/j.jaci.2012.05.050>
- 706 Munk, L. M., Hild, A. L., & Whitson, T. D. (2002). Rosette recruitment of a rare en-
707 demic forb (*Gaura neomexicana* subsp. *coloradensis*) with canopy removal of associ-
708 ated species. *Restoration Ecology*, 10(1), 122–128. [https://doi.org/10.1046/j.1526-100X.2002.10113.x](https://doi.org/10.1046/j.1526-
709 100X.2002.10113.x)
- 710 Nei, M., Maruyama, T., & Chakraborty, R. (1975). The Bottleneck Effect and Genetic
711 Variability in Populations. *Evolution*, 29(1), 1–10.
- 712 Nguyen, V., Buckley, Y. M., Salguero-Gómez, R., & Wardle, G. M. (2019). Conse-
713 quences of neglecting cryptic life stages from demographic models. *Ecological Mod-
714 ellling*, 408(June). <https://doi.org/10.1016/j.ecolmodel.2019.108723>

- 715 Oksanen, J., Blanchet, F. G., Friendly, M., Kindt, R., Legendre, P., McGlinn, D., Minchin,
716 P. R., O'Hara, R. B., Simpson, G. L., Solymos, P., Stevens, M. H. H., Szoecs, E., &
717 Wagner, H. (2020). *vegan: Community Ecology Package*. R package version 2.5-7.
718 Retrieved from <https://cran.r-project.org/package=vegan>
- 719 Paniw, M., Quintana-Ascencio, P. F., Ojeda, F., & Salguero-Gómez, R. (2017). Accounting
720 for uncertainty in dormant life stages in stochastic demographic models. *Oikos*, 126(6),
721 900–909. <https://doi.org/10.1111/oik.03696>
- 722 Pfister, C. A. (1998). Patterns of variance in stage-structured populations : Evolutionary
723 predictions and ecological implications. *Proceedings of the National Academy of
724 Sciences*, 95(January), 213–218.
- 725 PRISM Climate Group; Oregon State University. (2021). *PRISM Climate Group, Oregon
726 State University*. Retrieved from <https://prism.oregonstate.edu>
- 727 Pulliam, H. R. (2016). Sources , Sinks , and Population Regulation Author (s) : H . Ronald
728 Pulliam Published by : The University of Chicago Press for The American Society of
729 Naturalists Stable URL : <http://www.jstor.org/stable/2461927> Accessed : 17-03-2016
730 21 : 27 UTC Your use. , 132(5), 652–661.
- 731 Rabinowitz, D. (1981). Seven forms of rarity. In H. Synge (Ed.), *The biological aspects of
732 rare plant conservation*. John Wiley & Sons, Ltd. <https://doi.org/10.2307/4110060>
- 733 Ramula, S., Rees, M., & Buckley, Y. M. (2009). Integral projection models perform better
734 for small demographic data sets than matrix population models: A case study of
735 two perennial herbs. *Journal of Applied Ecology*, 46(5), 1048–1053. <https://doi.org/10.1111/j.1365-2664.2009.01706.x>
- 737 Rees, M., Childs, D. Z., Metcalf, C. J. E., Rose, K. E., Sheppard, A. W., & Grubb, P. J.
738 (2006). Seed dormancy and delayed flowering in monocarpic plants: selective interactions
739 in a stochastic environment. *The American Naturalist*, 168(2), E53-E71.
740 <https://doi.org/10.1086/505762>
- 741 Rosenzweig, M. L., & Lomolino, M. V. (1997). The Biology of Rarity. In W. E. Kunin &
742 K. J. Gaston (Eds.), *The biology of rarity*. London: Chapman & Hall. https://doi.org/10.1007/978-94-011-5874-9_7
- 744 Rovere, J., & Fox, J. W. (2019). Persistently rare species experience stronger negative fre-

- 745 quency dependence than common species: A statistical attractor that is hard to avoid.
746 *Global Ecology and Biogeography*, 28(4), 508–520. <https://doi.org/10.1111/geb.12871>
- 747 Säterberg, T., Jonsson, T., Yearsley, J., Berg, S., & Ebenman, B. (2019). A potential role for
748 rare species in ecosystem dynamics. *Scientific reports*, 9(1), 11107. <https://doi.org/10.1038/s41598-019-47541-6>
- 750 Sgarbi, L. F., & Melo, A. S. (2018). You don't belong here: explaining the excess of rare
751 species in terms of habitat, space and time. *Oikos*, 127(4), 497–506. <https://doi.org/10.1111/oik.04855>
- 753 Spear, M. J., Walsh, J. R., Ricciardi, A., & Vander Zanden, M. J. (2021, 4). *The Invasion
754 Ecology of Sleeper Populations: Prevalence, Persistence, and Abrupt Shifts* (Vol. 71)
755 (No. 4). Oxford University Press. <https://doi.org/10.1093/biosci/biaa168>
- 756 Stanley, S. M. (1979). *Macroevolution: Pattern and Process*. W. H. Freeman.
- 757 Tuljapurkar, S. (1989). An Uncertain Life : Demography in Random Environments in
758 population analysis but it ignores variation in population vital rates (i . e .,. *Population
759 (English Edition)*, 294, 227–294.
- 760 Venables, W. N., & Ripley, B. D. (2002). *Modern Applied Statistics with S* (Fourth ed.).
761 New York: Springer. Retrieved from <https://www.stats.ox.ac.uk/pub/MASS4/>
- 762 Villellas, J., Doak, D. F., García, M. B., & Morris, W. F. (2015). Demographic compensation
763 among populations: What is it, how does it arise and what are its implications? *Ecology
764 Letters*, 18(11), 1139–1152. <https://doi.org/10.1111/ele.12505>
- 765 Vitalis, R., Glémin, S., & Olivieri, I. (2004). When genes go to sleep: The population genetic
766 consequences of seed dormancy and monocarpic perenniability. *American Naturalist*,
767 163(2), 295–311. <https://doi.org/10.1086/381041>
- 768 Wagner, W. L., Hoch, P. C., & Raven, P. H. (2007). *Revised Classification of the On-
769 agraceae* (Vol. 83). The American Society of Plant Taxonomists. Retrieved from
770 <http://link.springer.com/10.1007/BF03027161>
- 771 William A Link, Paul F Doherty, Fr. (2002). Scaling in sensitivity analysis. *Ecology*, 83(12),
772 3299–3305.

773 S1 Supplementary Materials**774 Species Information**

775 *Oenothera coloradensis* seeds are contained within small, woody, indehiscent capsules that
776 contain 2-5 seeds each (Burgess et al., 2005). A single adult individual can produce >500 capsules.
777 This species does not reproduce vegetatively, although seeds typically germinate near the base
778 of the parent plant, which often results in dense clumps of vegetative individuals (Heidel et al.,
779 2021). *O. coloradensis* has no known specialist pollinators or seed dispersers (Floyd & Ranker,
780 1998; Heidel et al., 2021). Previous work established that *O. coloradensis* population growth rate
781 is particularly impacted by recruitment of seedlings (Floyd & Ranker, 1998). Recruitment increases
782 when non-*O. coloradensis* community biomass is removed, indicating that surrounding grasses and
783 forbs outcompete or shade-out seedlings (Munk et al., 2002).

784 *O. coloradensis* commonly co-occurs with *Agrostis stolonifera*, *Pascopyrum smithii*, *Poa pratensis*,
785 *Glycyrrhiza lepidota*, *Iris missouriensis*, *Cirsium flodmanii*, and *Grindelia squarrosa* (Jennings,
786 2000; Munk et al., 2002). Encroachment of woody shrubs such as *Salix exigua* has been correlated
787 with declining numbers in some populations (Heidel et al., 2021).

788 The Wyoming Natural Diversity Database (WYNDD) began a base-wide census of reproductive
789 individuals in the FEWAFB population in 1986, and has repeated this census annually since 1988
790 (Heidel et al., 2021). The first estimate of species size after its full geographic range was identified
791 occurred in 1998, when it was approximated that the entire species consisted of 47,300 to 50,300
792 reproductive individuals.

Table S1: Permanent Plot Locations and subpopulation-level sample sizes for each year and individual type (seedling vs. non-seedling). GPS coordinates listed in decimal degrees, map datum and spheroid: WGS 84.

Site	Subpopulation	Plot	N Name	W Coord.	W Coord.	Sample Size					
						2018		2019		2020	
						non-seedling	seedling	non-seedling	seedling	non-seedling	seedling
FEWAFB	Unnamed Creek	U3	41.13642	-104.87209							
	Unnamed Creek	U4	41.13634	-104.87183		740	525	528	417	406	530
	Unnamed Creek	U6	41.13647	-104.87132							
	Diamond Creek	D7	41.14340	-104.88380							
	Diamond Creek	D10	41.14441	-104.88303		235	209	347	149	275	81
	Diamond Creek	D11	41.14431	-104.88094							
	Crow Creek	C4	41.15540	-104.87497							
	Crow Creek	C5	41.15477	-104.87474		203	127	214	98	150	160
	Crow Creek	C8	41.15534	-104.87487							
Soapstone	Pasture HQ5	S1	40.99297	-105.00925							
	Pasture HQ5	S2	40.99318	-105.00935		283	772	714	813	641	423
	Pasture HQ5	S3	40.99342	-105.00937							
	Pasture HQ3	S4	40.98623	-105.01691							
	Pasture HQ3	S5	40.98639	-105.01671		102	138	158	173	117	104
	Pasture HQ3	S6	40.98650	-105.01656							
	Meadow	S7	40.98753	-105.02148							
	Meadow	S8	40.98747	-105.02179		44	31	47	28	48	12
	Meadow	S9	40.98724	-105.02145							

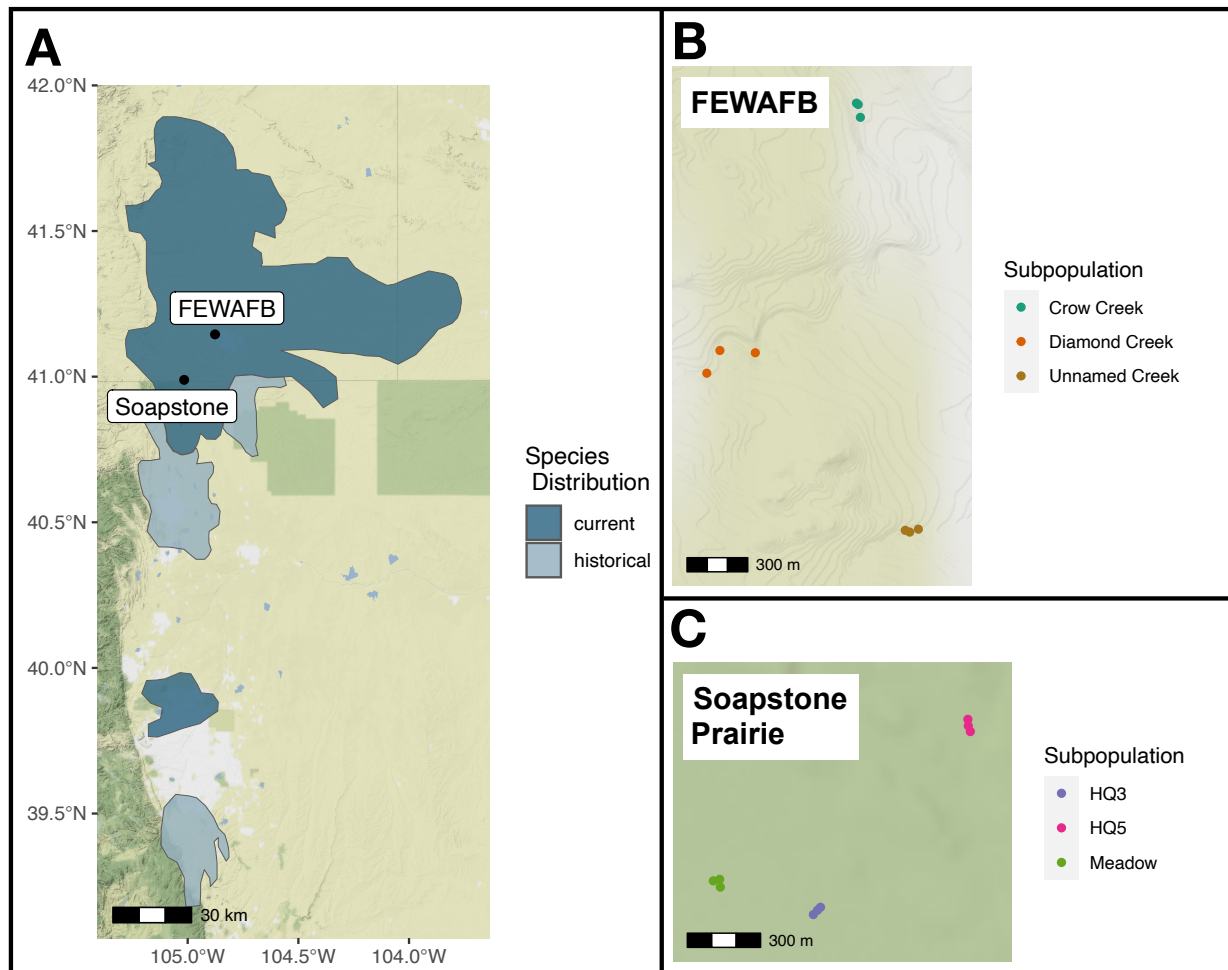


Figure S1: **A** The current known distribution of *O. coloradensis*, shown in dark blue, extends into Wyoming, Colorado, and Nebraska. The historical distribution included the current distribution area as well as some additional locations shown in pale blue. Distribution information comes from Everson, 2019. Black dots show the relative location of the FEWAFB and Soapstone prairie populations included in this study. Colored dots show the location of plots in each subpopulation at FEWAFB (**B**) and Soapstone Prairie (**C**).

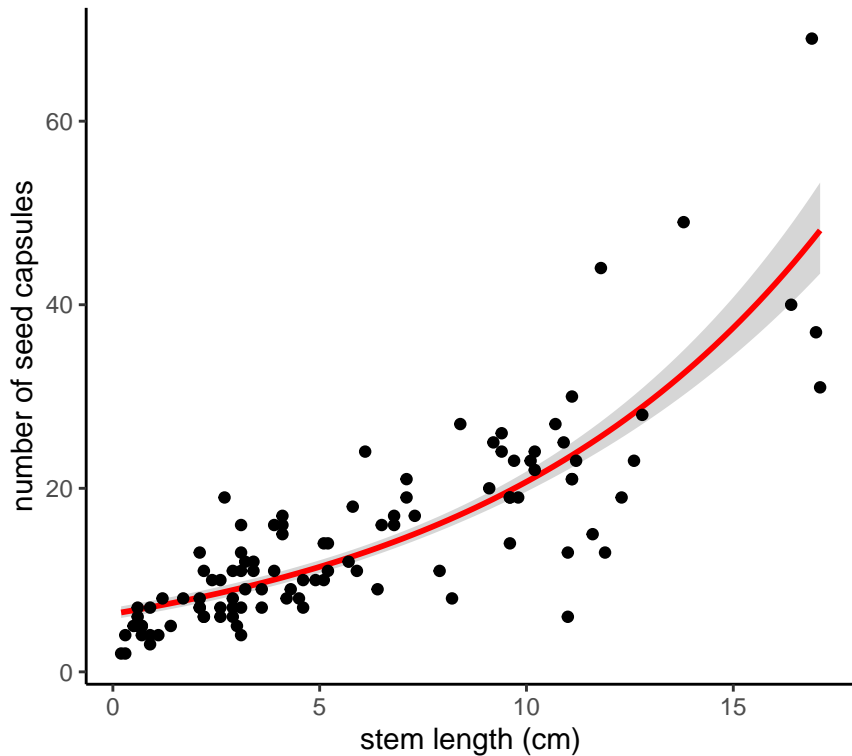


Figure S2: As the stem length of an *Oenothera coloradensis* flowering individual increases, the number of capsules it produces increases as well. The red line shows the fit from a Poisson generalized linear model, and the grey ribbon shows the 95% confidence interval around the fitted relationship. Model equation: Number of capsules = $e^{(1.843+0.119 \times S)}$, where S is stem length in cm (pseudo R-squared = 0.42, $P = < 0.01$, Residual deviance = 186.98, df = 104).